

# SCIENTIFIC REPORTS



OPEN

## Tightening slip knots in raw and degummed silk to increase toughness without losing strength

Maria F. Pantano<sup>1</sup>, Alice Berardo<sup>1</sup> & Nicola M. Pugno<sup>1,2,3</sup>

Received: 03 July 2015

Accepted: 04 November 2015

Published: 12 February 2016

**Knots are fascinating topological elements, which can be found in both natural and artificial systems. While in most of the cases, knots cannot be loosened without breaking the strand where they are tightened, herein, attention is focused on slip or running knots, which on the contrary can be unfastened without compromising the structural integrity of their hosting material. Two different topologies are considered, involving opposite unfastening mechanisms, and their influence on the mechanical properties of natural fibers, as silkworm silk raw and degummed single fibers, is investigated and quantified. Slip knots with optimized shape and size result in a significant enhancement of fibers energy dissipation capability, up to 300–400%, without affecting their load bearing capacity.**

Knots are intriguing topological elements, with a variety of examples appearing in fine arts (Fig. 1a) as well as many scientific fields, including mathematics<sup>1</sup>, polymer science<sup>2,3</sup>, colloids<sup>4,5</sup>, fluids<sup>6</sup>, chemistry<sup>7,8</sup>, biology<sup>9</sup>, and obviously engineering<sup>10</sup>. Knots can be introduced by human hand<sup>11</sup>, but many biological systems, like proteins and DNA, naturally form knotted configurations<sup>12</sup>, with their function being still mysterious and under debate<sup>13</sup>. Herein, we investigate how the presence of knots is able to affect the mechanical properties of natural fibers, as silkworm silk. Indeed, it has been recently proposed that knots can significantly improve the energy dissipation capability (i.e., toughness) of materials<sup>10</sup>.

Silkworm silk has been implemented for centuries in textile and medical industries, with recent application in composites<sup>16</sup>, tissue engineering scaffolds<sup>17,18</sup> and drug delivery<sup>19</sup>, and is now receiving a renewed interest, as natural materials can address the need for sustainable and biodegradable structural components<sup>20</sup>.

Thus, we exploit potential knotted structures to artificially increase the toughness of silkworm silk without any genetic modification or chemical treatment, but reproducing at the microscale the same toughening function which sacrificial bonds have in highly coiled macromolecules<sup>14,15</sup>. In fact, as the breakage of weak bonds (i.e., sacrificial bonds) reveals a hidden length in macromolecules, which can thus be further stretched without breaking their backbones, the knots release in our samples provide additional length to silk fibers, which can thus be further elongated before failure.

From a mechanical point of view, silk fibers extracted from silkworm cocoons have been reported with remarkable mechanical properties, i.e., Young modulus up to 16 GPa<sup>21</sup>, fracture strength up to 600 MPa<sup>22</sup> and toughness of  $6 \cdot 10^4$  J/kg<sup>23</sup>, even though these cannot compete with those characterizing spider silk dragline<sup>24</sup>, having fracture strength of 1.3 GPa and toughness of  $16 \cdot 10^4$  J/kg<sup>23</sup>. However, since spiders offer a significantly smaller yield capability, which hinders their silk to be fully implemented in a massive industrial production<sup>25</sup>, it would be desirable to combine the advantages offered by both such biomaterials, thus developing methods to provide silkworm silk with spider silk performances. Apart from genetic modification and chemical treatment<sup>26,27</sup>, mechanical properties of silkworm silk were showed to be improvable by artificially increasing the reeling speed of silk from the silkworm<sup>23</sup>.

In the present paper, we focus on a knot-based strategy<sup>10</sup> to improve the toughness of as-produced silkworm silk. Our strategy<sup>10</sup> requires the introduction within single silk fibers of a sliding frictional element, namely a knot with a proper topology and optimized shape and size.

While knots typically encountered in biological or chemically synthesized molecular systems cannot be loosened without breaking (chemically or mechanically) the strand where they are tightened, with only rare exceptions<sup>28</sup>, the knots introduced in our fibers were designed as able to unfasten as their opposite ends are pulled apart.

<sup>1</sup>Laboratory of Bio-inspired & Graphene Nanomechanics, Department of Civil, Environmental and Mechanical Engineering, University of Trento, Via Mesiano 77, 38123 Trento, Italy. <sup>2</sup>Center for Materials and Microsystems, Fondazione Bruno Kessler, Via Sommarive 18, 38123 Povo (TN), Italy. <sup>3</sup>School of Engineering and Materials Science, Queen Mary University of London, Mile End Road, London E1 4NS, U.K. Correspondence and requests for materials should be addressed to N.M.P. (email: nicola.pugno@unitn.it)

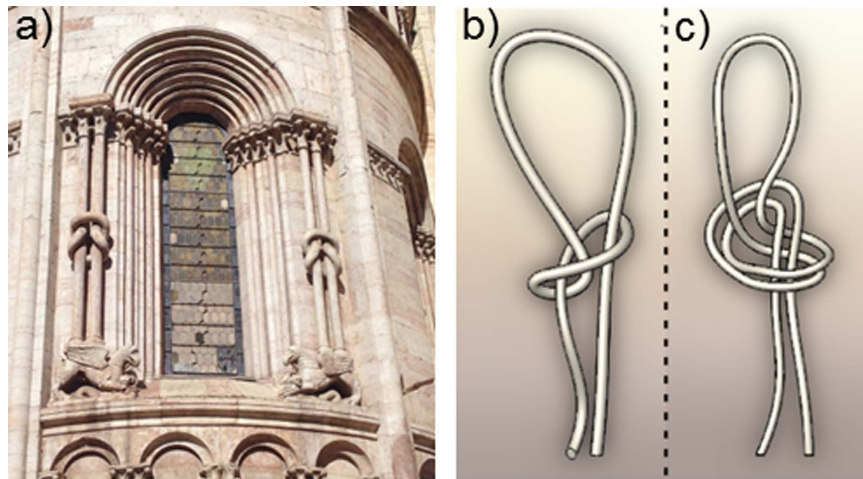


**Figure 1.** (a) Duomo of Trento (Italy): detail of the apse loggia with a couple of knotted columns (XIII century). Photograph by A.B. Schematics of the knots designed in our experiments on single silk fibers: the single turned slip knot, STSK, (b) and the double turned slip knot, DTSK, (c) where the fiber is turned either once or twice at the bottom of a loop.

In fact, this is a necessary condition to fully exploit the knot friction potential and avoid any stress concentration, which can trigger premature failure of the fiber, thus compromising its load bearing capacity.

Hereby, in the present study attention was focused on slip or running knots. In particular, two different topologies involving opposite unfastening mechanisms were implemented and optimized in case of single silk fibers (Fig. 1b,c). Furthermore, since silk extracted directly from cocoons usually undergoes a degumming process before being processed in industrial applications, in our knot optimization we considered both natural (i.e., extracted directly from a cocoon) and degummed (i.e., extracted from degummed cocoons) fibers, in order to capture potential differences due to the different surface friction coefficients. Then, tensile tests were performed on both knotted and unknotted control samples in order to evaluate the toughness enhancement due to the knot presence.

## Results

In the present experiments, we compared the effectiveness of two kinds of slip (or running) knots, where the fiber was turned either once (single turned slip knot, STSK, also known as *noose*) or twice (double turned slip knot, DTSK, also known as *overhand loop*) at the bottom of a loop (Fig. 2). In both cases, the fiber is allowed to slide throughout the knot, in order to promote energy dissipation, but undergoes a different unfastening mechanism. In fact, while the first kind of knot is always able to unfasten, even when extremely tight, as it loosens when the fiber ends are pulled apart, the second one poses much more issues, since, on the contrary, it becomes tighter as the fiber is pulled. For both untreated and degummed silk, either knot topologies were optimized in order to fulfill two main requirements. First, the knot has to be sufficiently tight in order to extend the strain interval where the fiber experiences a relatively high stress. Second, this must be able to unfasten as the fiber opposite ends are pulled apart, in order to not affect the fiber fracture strength.

Reference values of silk toughness were derived from tensile testing of control untreated baves and degummed single silk fibers with no knot implemented (i.e., toughness is proportional to the area under sample stress-strain curve) (Fig. 3). Then, in order to evaluate the toughness increase due to the knot introduction, we performed a wide experimental campaign, with the corresponding results reported in the Supplementary Information.

However, extracting meaningful data from tensile tests on silk is not straightforward. In fact, as expected from the literature, the stress-strain curves of control silk fibers showed significant variability (Fig. 3), which causes in turn variability in terms of mechanical properties, included toughness. Such variability is mainly caused by fluctuations in the fiber diameter, which is in turn dependent of many factors closely related to the silkworm nature<sup>29</sup>, such as mode and speed of the spinning process. Furthermore, fiber diameter can not only vary in size<sup>20,22</sup> but also in shape over the same cocoon<sup>21</sup>. However, as common practice in the literature<sup>21</sup>, we considered the fibers as provided with a circular cross-section.

The diameter of each tested fiber was evaluated from observation under either optical or scanning electron (SEM) microscope, providing average values of 21  $\mu\text{m}$  and 12  $\mu\text{m}$  for natural and degummed fibers, respectively.

For a fiber without any knot, the energy dissipated per unit mass,  $T_u$ , e.g., toughness modulus, can be computed from its stress-strain curve as (Fig. 4a):

$$T_u = 1/m \int_0^{x_f} F dx = Al/m \int_0^{\varepsilon_f} \sigma d\varepsilon = 1/\rho \int_0^{\varepsilon_f} \sigma d\varepsilon \quad (1)$$

where  $m$  is the fiber mass,  $x_f$  is the displacement at fracture,  $F$  is the applied force,  $A$  is the fiber cross sectional area,  $l$  is the fiber initial length,  $\rho$  is the volumetric density,  $\varepsilon_f = (l_f - l)/l = x_f/l$  is the fracture strain,  $l_f$  is the fiber final length, and  $\int_0^{\varepsilon_f} \sigma d\varepsilon$  is the area under the stress-strain curve. Such expression has to be slightly adjusted if

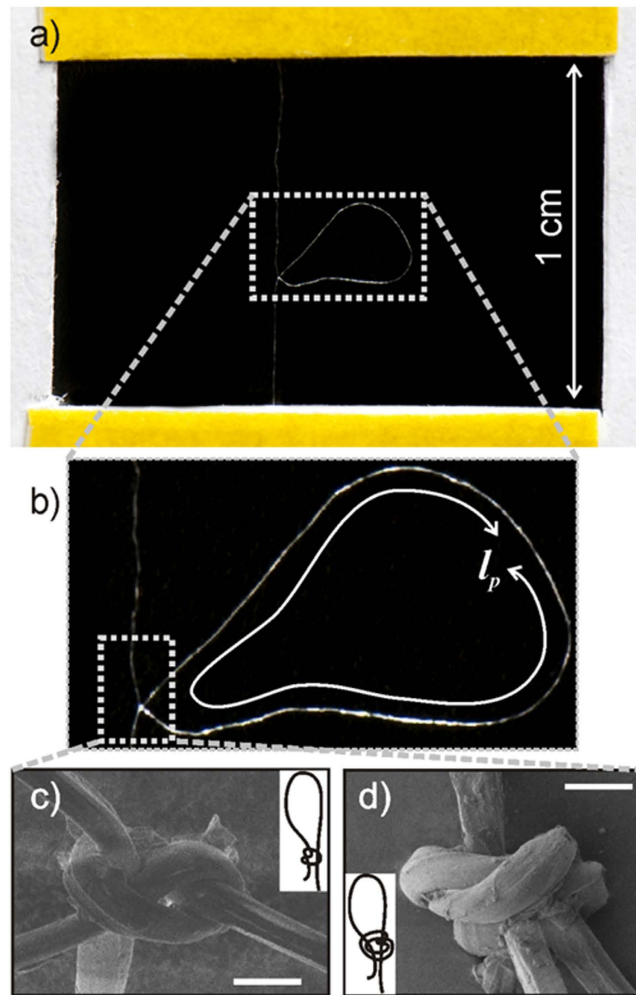


**Figure 2.** (a) A degummed silk fiber, provided with an optimized knot, spanning over a paper frame prepared for nanotensile testing. The knot, either single (STSK) or double (DTSK) turned slip knot, is characterized by two main parameters, the loop length,  $l_p$ , and the knot diameter, as shown in the zoomed view (b). SEM images of the single (c) and double (d) turned slip knot. Scale bars: 20  $\mu\text{m}$ .

knotted fibers are instead considered. In fact, if a knotted fiber with still length  $l$  is tested (Fig. 4b), its toughness modulus can be computed as:

$$T_k = 1/m \int_0^{x_f^*} F dx = Al_0/m \int_0^{\varepsilon_f^*} \sigma d\varepsilon = (1 - k_1)/\rho \int_0^{\varepsilon_f^*} \sigma d\varepsilon \quad (2)$$

where  $x_f^* = l - l_0 + x_f$ ,  $l_0$  is the initial length equal to the distance between the fiber opposite ends (Fig. 4b),  $\varepsilon_f^* = x_f^*/l_0$ , and  $k_1 = (l - l_0)/l$  accounts for the difference between  $l_0$  and  $l^{10}$ .

In order to derive quantitative results of knot induced toughness increase, which is not affected by variability of silk mechanical properties, we pursued the following strategy when comparing the toughness of a knotted sample computed according to Eq. (2) with the toughness of a control sample calculated according to Eq. (1). In fact, when possible, we referred toughness comparison to the same fiber; alternatively, as reference value we considered the toughness of an unknotted fiber which was extracted from a cocoon region adjacent to that of the knotted fiber, thus expecting a minimal variation in their physical and mechanical properties.

In fact, in some cases, after a series of loading and unloading events due to knot fastening and unfastening, the knot loosens completely, leaving the stress-strain curve of knotted fibers collapsing to the stress-strain curve of the corresponding unknotted samples, as shown in Fig. 4. This indicates that the mechanical behavior of silk is not affected by loading-unloading cycles, confirming previous results derived from dynamic tests<sup>22</sup> and allowing the final part of the curve (highlighted in Fig. 4b) to be considered as the stress-strain curve related to the unknotted configuration of the same fiber. In such situation, the ratio between the toughness of the knotted fiber,  $T_k$ , and the toughness of the corresponding unknotted fiber,  $T_u$ , was computed as:

$$T_k/T_u = \left[ Al_0/m \int_0^{\varepsilon_f^*} \sigma d\varepsilon \right] / \left[ Al_0/m \int_{\varepsilon^*}^{\varepsilon_f^*} \sigma d\varepsilon \right] = \int_0^{\varepsilon_f^*} \sigma d\varepsilon / \int_{\varepsilon^*}^{\varepsilon_f^*} \sigma d\varepsilon \quad (3)$$

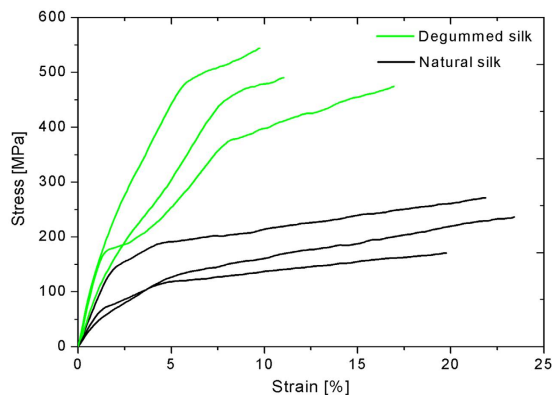


**Figure 3.** Stress-strain curves derived from tensile tests carried out on single untreated baves (black line) and degummed fibers (green line), both showing significant variability.

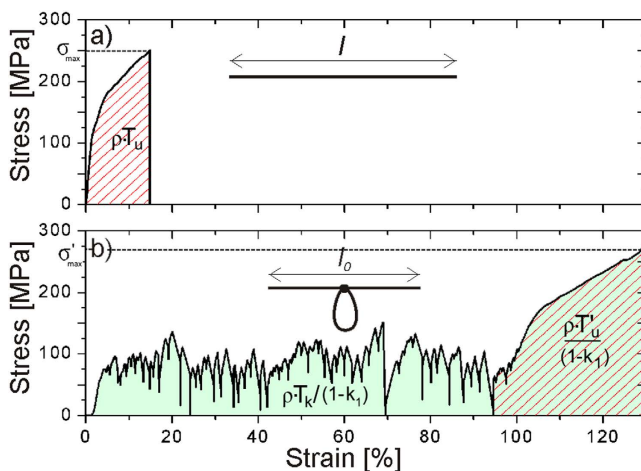


**Figure 4.** (a) Stress-strain curve of an unknotted natural fiber with length  $l$  and toughness modulus  $T_u$  (equal to the marked area divided by the fiber density  $\rho$ ). (b) Stress-strain curve of a knotted natural fiber with length  $l_0$ , toughness modulus  $T_k$  (equal to the shadowed area multiplied by  $(1-k_1)/\rho$ , where  $k_1=1-l_0/l$ ), which was extracted from a cocoon region adjacent to the unknotted fiber (a). The presence of the knot modifies the shape of the stress-strain curve (a), introducing a plastic-like plateau and leaving the final region (marked with lines and equal to  $T_u'$ , the fiber toughness modulus after knot release, multiplied by  $\rho/(1-k_1)$ ) almost corresponding to the stress-strain curve of the same fiber with unknotted configuration. The strain interval within this final region appears larger than in (a) since it is computed with respect to  $l_0$  instead of  $l$ .

where  $\int_{\varepsilon^*}^{\varepsilon_f} \sigma d\varepsilon$  is the area under the final part of the stress-strain curve, where the knot is completely released.

In other tests, the stress-strain curve of knotted fibers showed a well-defined plateau up to the end (as the curve corresponding to a natural fiber provided with single turned slip knot reported in Fig. 5a). Hereby, it is not possible to identify the final region of the stress-strain curve as the stress-strain curve corresponding to a plain sample. Then, we derived a reference toughness value from testing an unknotted fiber initially adjacent to the fiber where knot was then implemented.

Thus, in order to compare toughness values of a knotted and corresponding unknotted fiber, the area under the stress-strain curve of the knotted fiber has to be scaled by the factor  $(1-k_1)$ :

$$T_k/T_u = \left[ (1 - k_1)/\rho \int_0^{\varepsilon_f^*} \sigma d\varepsilon \right] / \left[ 1/\rho \int_0^{\varepsilon_f} \sigma d\varepsilon \right] = (1 - k_1) \int_0^{\varepsilon_f^*} \sigma d\varepsilon / \int_0^{\varepsilon_f} \sigma d\varepsilon, \quad (4)$$

where the symbols have the same meaning as before. Results obtained for both  $T_u'$  and  $T_u$  are reported in Table 1.

In the presented analysis, the toughness increase was evaluated according to expression (3) for degummed fibers provided with either single or double turned slip knot and natural fibers provided with double turned slip knot. Expression (4) was used instead in most of the cases to evaluate the toughness increase in natural fibers with single turned slip knot.

Figure 5a,b reports example stress-strain curves derived for natural and degummed single silk fibers with optimized single or double turned slip knot.

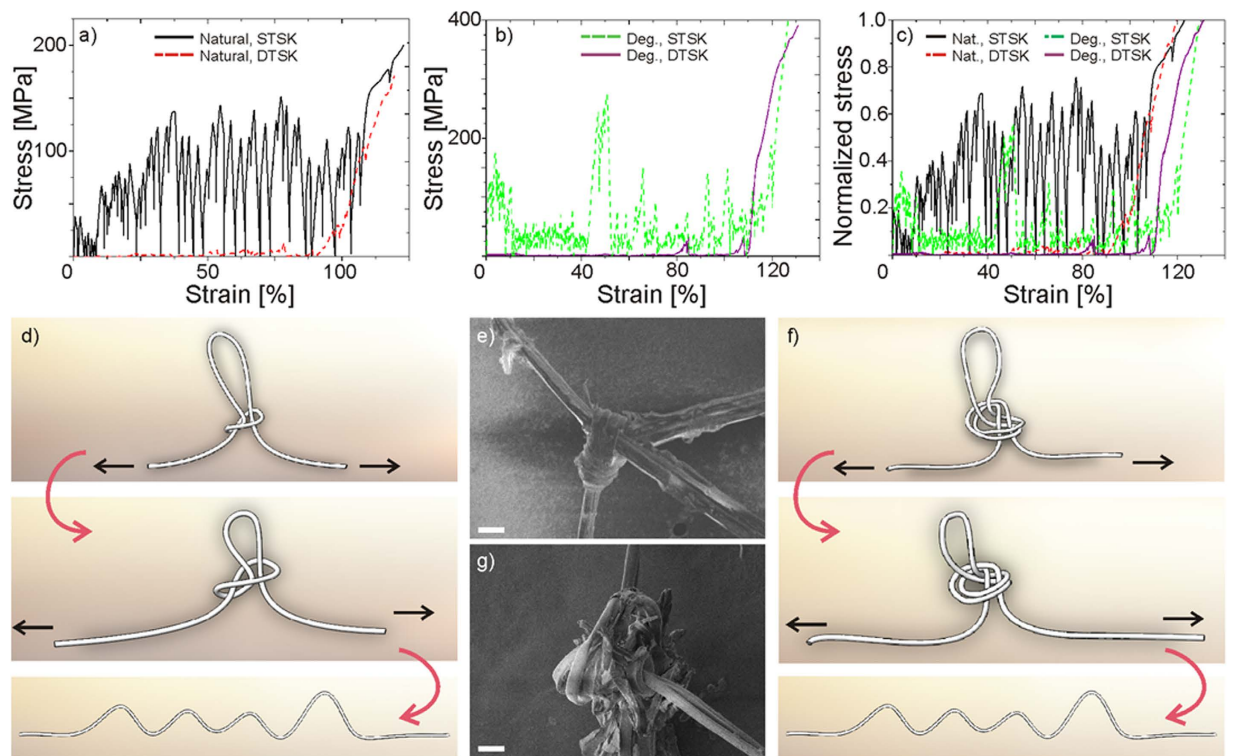


**Figure 5. Stress-strain curves of natural (a,b) degummed silk fibers with optimized single or double turned slip knot. (c) Comparison between the normalized stress-strain curves obtained for natural and degummed single silk fibers provided with optimized knots. Stress values are normalized with respect to fracture strength. (d) Unfastening mechanism of the single turned slip knot, which tends to loosen as the fiber ends are pulled apart. Such knot can always be released, even when extremely tight, as shown in the SEM image (e). (f) Unfastening mechanism of the double turned slip knot, which tends to further tie as the fiber ends are pulled apart. Thus, if this knot is too tight at the beginning of the test, it cannot be released, as occurred in the natural silk fiber reported in the SEM image (g) which broke at the knot entrance. The sericin coating looks significantly damaged by friction. Scale bars: 30  $\mu\text{m}$ .**

With respect to unknotted control samples (Fig. 3), many differences emerge. First, as expected, the knot presence extends the strain interval (i.e., fibers provided with a knot reach a bigger apparent strain) and introduces an artificial plateau, characterized by a series of peaks and drops, corresponding to partial fastening and unfastening of the fiber in the knot and related stick-slips. In particular, a well-defined plastic-like plateau appears especially when the single turned slip knot topology is considered and this is more evident for natural fibers than for degummed fibers. This means that natural fibers with this knot topology can be constantly high stressed throughout the whole test, causing energy dissipation to be strongly enhanced. Such observations are quantitatively confirmed by values reported in Table 1.

In fact, the single turned slip knot topology allowed to significantly enhance toughness of both natural and degummed fibers, with more than 350% and 250% increase in the optimal configuration, respectively. On the contrary, the double turned slip knot topology resulted to be sensibly less performing, with comparable toughness increase around 110% for both natural and degummed fibers.

## Discussion

The results shown in the previous section can be explained looking at the unfastening mechanism involved in either knot topology. In fact, the single turned slip knot tends to loosen during the test (Fig. 5d). Hereby, it is possible to start from a very tight configuration (Fig. 5e), which provides the fiber to be significantly stressed throughout the whole test within a relatively wide apparent strain interval, which allows to more than quadrupling toughness (see Supplementary Information). On the contrary, the double turned slip knot tends to further tie as the fiber is pulled (Fig. 5f). Thus, in order to release completely the fiber without any damage, it is necessary to start from a very loose configuration. This, however, causes the fiber not to be very stressed, except at the end of the test, providing a much less significant toughness enhancement.

On average, with reference to the single turned slip knot, higher toughness values were reported for natural silk than for degummed silk. This is related to the possibility for natural fibers to dissipate more energy by friction, thus reaching a stress plateau much closer to their fracture strength, as it emerges if the stress values reported in Fig. 5a,b are normalized with respect to the corresponding fracture strength (Fig. 5c). The double turned slip knot topology provided instead comparable results for both natural and degummed fibers.

	Diameter [μm]	Strength of unknotted fibers [MPa]	Toughness modulus of reference unknotted fiber, $T_u$ [J/g]	Knot topology	Strength [MPa]	Toughness modulus, $T_k$ [J/g]	Toughness modulus after unfastening, $T_u'$ [J/g]	Friction stress/strength
Raw silk	21 ± 2	219 ± 68	20 ± 11	STSK	229 ± 50	45 ± 12	15 ± 9	> 8 %
					216 ± 46	19 ± 8	16 ± 7	< 8 %
				DTSK	–	–	–	> 8 %
					237 ± 53	17 ± 18	16 ± 8	< 8 %
Degummed silk	12 ± 2	502 ± 141	28 ± 12	STSK	343 ± 104	28 ± 9	11 ± 7	> 8 %
					463 ± 120	36 ± 18	28 ± 19	< 8 %
				DTSK	–	–	–	> 8 %
					434 ± 146	29 ± 17	27 ± 17	< 8 %

**Table 1.** Strength or toughness ( $T_u$ ) of control unknotted fibers. Toughness modulus ( $T_k$ ), strength or toughness modulus after unfastening ( $T_u'$ ) of knotted fibers with single turned slip knot (STSK) or double turned slip knot (DTSK) topologies. For each knot topology, two sets of data are provided, corresponding to samples with average stress in the strain interval 0% - 40% of their strain at break (i.e., friction stress) above or below the 8% of their strength. Such threshold value was considered as the minimum friction stress required for knots to be efficiently implemented.

Such different behavior can be explained considering the role played by sericin coating. In fact, due to sericin, natural silk fibers are less smooth than degummed fibers, thus being more prone to friction as they run through the knot. However, when the knot is always able to unfasten (e.g., STSK), this is an added value and contributes favorably to further increase the fiber toughness. On the other side, when it is difficult for the fiber to run throughout its loop as the knot tends to tie during tensile tests (e.g., DTSK), any additional friction source can further hinder sliding, causing damage and premature failure of the fiber (Fig. 5e–g). Thus, it is necessary to start from a very loose configuration, which minimizes or even cancels out the beneficial effect of sericin on friction enhancement.

## Conclusions

In summary, we have presented the effect of slip knots on the toughness of single silkworm silk fibers applying the strategy proposed in ref [10]. Our study demonstrates that, under optimized conditions, a slip knot introduced within the fiber can increase its energy dissipation capability, without causing significant damage to it and avoiding significant stress concentration at the knot entrance. Here, two different topologies were considered, with the fiber turned either once or twice at the bottom of a loop. While both topologies allow the fiber to slide within their loop, thus promoting energy dissipation, they involve a different unfastening mechanism, with the knot prone to either untie or tie, as the fiber ends are pulled apart. The first topology with the fiber turned once at the bottom of a loop provided the best results, with more than three times toughness enhancement compared to a reference unknotted sample.

We believe that the silk toughness could be further increased by considering longer loop to fiber length ratio than that of our experiments, or introducing multiple slip knots within the same fiber. Thus, the results presented in our work should serve as a guide for future investigation of more complex knots, like those implemented in textile industry, in order to provide new tools for optimizing systems where energy dissipation is highly requested.

## Methods

**Sample preparation.** For the experiments presented in the present paper, single silk fibers were extracted from untreated and degummed cocoons of domestic *Bombyx mori* silkworm. Some of the isolated fibers were manipulated by tweezers in order to introduce a knot, while the others were left plain and used as control samples. From a structural point of view, natural silk fibers (baves) are composed of two filaments (known in the literature as brins), mainly consisting of fibroin, which are coated with a sericin layer binding them together. Since sericin does not contribute to load bearing capacity of the bave<sup>30</sup>, this was removed through a typical degumming process<sup>31</sup>, thus allowing to obtain bare fibroin fibers separated one from another. The process implemented in the present experiments followed a typical procedure<sup>31</sup>, consisting of boiling twice the cocoon with 1.1 g/L and 0.4 g/L  $\text{Na}_2\text{CO}_3$  (anhydrous, minimum 99%, from Sigma Aldrich) water solution for one hour each time. This allowed to remove any sericin traces, obtaining bare fibroin fibers, which were then washed against distilled water and air-dried.

Some samples were left plain and used as control samples, while others were provided with either single or double turned slip knots. Starting from a fiber length ( $l$ ) of 20 mm and a distance between the fiber ends ( $l_0$ ) of 10 mm, the optimal single turned slip knot geometry which allowed to maximize the fiber energy dissipation capability had a very small knot diameter with a loop length ( $l_p$ ) of about 10 mm (Fig. 2). In fact, as this kind of knot tends to loosen during tensile tests, it is convenient to start from the tightest possible configuration. On the contrary, it was not possible to perform successful experiments with a fiber length of 20 mm and  $l_0$  equal to 10 mm, provided with double turned slip knot. In fact, knots with this size could not completely unfasten during tensile tests. Thus, an optimization process was carried out in order to guarantee the knot to completely release during a test on a fiber with the longest possible loop (for dissipating the highest possible energy), still keeping  $l_0 = 10$  mm.

This had the following geometry: knot diameter of  $6 \pm 0.3$  mm (with about 12 mm of fiber involved within the knot), and loop length ( $l_p$ ) of 6 mm.

**Tensile tests.** Both untreated baves and degummed single silk fibers were tested at room temperature through a nanotensile testing machine (Agilent T150 UTM) and at a strain rate of  $0.001 \text{ s}^{-1}$  in case of control samples and  $0.002 \text{ s}^{-1}$  in case of samples provided with knots.

## References

- Anstee, R. P., Przytycki, J. H. & Rolfsen, D. Knot Polynomials and Generalized Mutation. *Topol Appl* **32**, 237–249 (1989).
- Bayer, R. K. Structure transfer from a polymeric melt to the solid state-Part III: Influence of knots on structure and mechanical properties of semicrystalline polymers. *Colloid Polym Sci* **272**, 910–932 (1994).
- Saitta, A. M., Soper, P. D., Wasserman, E. & Klein, M. L. Influence of a knot on the strength of a polymer strand. *Nature* **399**, 46–48 (1999).
- Tkalec, U., Ravnik, M., Copar, S., Zumer, S. & Musevic, I. Reconfigurable Knots and Links in Chiral Nematic Colloids. *Science* **333**, 62 (2011).
- Sennyuk, B. *et al.* Topological colloids. *Nature* **493**, 200–205 (2013).
- Kleckner, D. & Irvine, W. T. M. Creation and dynamics of knotted vortices. *Nat. Phys.* **9**, 253–258 (2013).
- Forgan, R. S., Sauvage, J. P. & Stoddart, J. F. Chemical Topology: Complex Molecular Knots, Links and Entanglements. *Chem Rev* **111**, 5434–5464 (2011).
- Ayme, J. F. *et al.* A synthetic molecular pentafoil knot. *Nat Chem* **4**, 15–20 (2012).
- Meluzzi, D., Smith, D. E. & Arya, G. Biophysics of Knotting. *Ann Rev Biophys* **39**, 349–366 (2010).
- Pugno, N. M. The “Egg of Columbus” for Making the World’s Toughest Fibres. *PlosOne* **9**, 4 (2014)
- Arai, Y. *et al.* Tying a molecular knot with optical tweezers. *Nature* **399**, 446–448 (1999).
- Dean, F., Stasiak, A., Koller, T. & Cozzarelli, N. Duplex DNA knots produced by Escherichia coli topoisomerase I. Structure and requirements for formation. *J Biol Chem* **260**, 4975–4983 (1985).
- He, C., Lamour, G., Xiao, A., Gsponer, J. & Li, H. Mechanically Tightening a Protein Slipknot into a Trefoil Knot. *J Am Soc Chem* (2014) doi: dx.doi.org/10.1021/ja503997h.
- Fantner, G. E. *et al.* Sacrificial Bonds and Hidden Length: Unraveling Molecular Mesostuctures in Tough Materials. *Biophys J* **90**, 1411–1418 (2006).
- Palmeri, M. J., Putz, K. W. & Brinson, L. C. Sacrificial Bonds in Stacked-Cup Carbon Nanofibers: Biomimetic Toughening Mechanisms for Composite Systems. *ACS NANO* **4** (7), 4256–4264 (2010).
- Ude, A. U., Ariffin, A. K. & Azhari, C. H. An Experimental Investigation on the Response of Woven Natural Silk Fiber/Epoxy Sandwich Composite Panels Under Low Velocity Impact. *Fiber Polym* **14** (1), 127–132 (2013).
- Jin, H. J. & Kaplan, D. L. Mechanism of silk processing in insects and spiders. *Nature* **424** (6952), 1057–1061 (2003).
- Meinel, A. J. *et al.* Optimization strategies for electrospun silk fibroin tissue engineering scaffolds. *Biomaterials*, **30**, 3058–3067 (2009).
- Hardy, J. G., Romer, L. M. & Scheibel, T. R. Polymeric materials based on silk proteins. *Polymer* **49**, 4309–4327 (2008).
- Colomban, P., Manh Dinh, H., Riand, J., Prinsloo, L. C. & Mauchamp, B. Nanomechanics of single silkworm and spider fibres: a Raman and micromechanical in situ study of the conformation change with stress. *J Raman Spectrosc* **39**, 1746–1749 (2008).
- Perez-Rigueiro, J., Viney, C., Llorca, J. & Elices, M. Mechanical properties of single-brin silkworm silk. *J Appl Polym Sci*, **75**, 1270–1277 (2000).
- Perez-Rigueiro, J., Viney, C., Llorca, J. & Elices M. J. Silkworm Silk as an Engineering Material. *J Appl Polym Sci* **70**, 2439–2447 (1998).
- Shao, Z. & Vollrath, F. Surprising strength of silkworm silk. *Nature* **418**, 741 (2002).
- Pugno, N. M., Cranford, S. W. & Buehler M. J. Synergetic Material and Structure Optimization Yields Robust Spider Web Anchorages. *Small* **9** (16), 2747–2756 (2013).
- Altman, H. G. *et al.* Silk-based biomaterials. *Biomaterials* **24**, 401–416 (2003).
- Heim, M., Keerl, D. & Scheibel, T. Spider Silk: From soluble protein to extraordinary fiber. *Angew Chem* **48**, 3584–3596 (2009).
- Wang, M., Jin, H. J., Kaplan, D. L. & Rutledge, G. C. Mechanical properties of electrospun silk fibers. *Macromolecules* **37**, 6856–6864 (2004).
- King, N. P., Yeates, E. O. & Yeates, T. O. Identification of rare slipknots in proteins and their implications for stability and folding. *J Mol Biol* **373**, 153–166 (2007).
- Zhao, H. P., Feng, X. Q. & Shi, H. J. Variability in mechanical properties of *Bombyx mori* silk. *Mater Sci Eng C* **27**, 675–683 (2007).
- Perez-Rigueiro, J., Elices, M., Llorca, J. & Viney, C. Tensile Properties of Silkworm Silk Obtained by Forced Silking. *J Appl Polym Sci* **82**, 1928–1935 (2001).
- Bonani, W., Maniglio, D., Motta, A., Tan, W. & Migliaresi, C. Biohybrid nanofiber constructs with anisotropic biomechanical properties. *J Biomed Mater Res B* **96B** (2), 276–286 (2011).

## Acknowledgements

The authors wish to thank Nello Serra from “Comunità don Milani” (Acqui, CS, Italy) for kindly supplying the silk cocoons used in the experiments. NMP is supported by the European Research Council (ERC StG Ideas 2011 BIHSNAM n. 279985 on “Bio-Inspired hierarchical super-nanomaterials”, ERC PoC 2013-1 REPLICAS n. 619448 on “Large-area replication of biological anti-adhesive nanosurfaces”, ERC PoC 2013-2 KNOTTOUGH n. 632277 on “Super-tough knotted fibres”), by the European Commission under the Graphene Flagship (WP10 “Nanocomposites”, n. 604391) and by the Provincia Autonoma di Trento (“Graphene Nanocomposites”, n. S116/2012-242637 and reg.delib. n. 2266).

## Author Contributions

N.M.P. designed and coordinated the study and helped in drafting the manuscript, M.F.P. and A.B. carried out the experimental tests and drafted the manuscript.

## Additional Information

**Supplementary information** accompanies this paper at <http://www.nature.com/srep>

**Competing financial interests:** The authors declare no competing financial interests.

**How to cite this article:** Pantano, M. F. *et al.* Tightening slip knots in raw and degummed silk to increase toughness without losing strength. *Sci. Rep.* **6**, 18222; doi: 10.1038/srep18222 (2016).



This work is licensed under a Creative Commons Attribution 4.0 International License. The images or other third party material in this article are included in the article's Creative Commons license, unless indicated otherwise in the credit line; if the material is not included under the Creative Commons license, users will need to obtain permission from the license holder to reproduce the material. To view a copy of this license, visit <http://creativecommons.org/licenses/by/4.0/>

## Supplementary Information

Supplementary Tables S1-S4 report the results obtained from tensile tests on both raw and degummed single silk fibers provided with Single Turned Slip Knot (STSK) and Double Turned Slip Knot (DTSK) topologies. In particular, a variety of data can be found, including the strength and the toughness modulus ( $T_k$ ) of knotted fibers, the toughness modulus of knotted samples computed after complete knot release ( $T_u'$ ), the toughness modulus of a reference unknotted fiber ( $T_u$ ) when  $T_u'$  could not be clearly identified. Toughness modulus values were computed considering a density of  $1.4 \text{ g/cm}^3$  [S1]. Supplementary Tables S1-S4 include also the values of the mean stress reached by samples over 0% - 40% of their strain at break. In fact, the average stress value reached by knotted fibers at the beginning of tensile tests is indicative of the friction force and thus of the tightness quality of implemented knot. The values of toughness modulus reported in the first or fifth row of Table 1 of the main text are computed as average over those values corresponding to samples which reached an average friction stress above the threshold value of 8% of the sample strength. Samples satisfying such requirement were highlighted in both Supplementary Table S1 and S3. On the contrary, the values of toughness modulus reported in the second or sixth row of Table 1 of the main text are computed as average over those values corresponding to samples which reached an average friction stress below the threshold. In case of DTSK, neither sample reached a friction mean stress above the threshold, thus demonstrating its low efficiency if compared to STSK topology.

Supplementary Table S1. Raw silk fibers with single turned slip knot: Strength, average friction stress/strength over 0% - 40% of the strain at break, toughness modulus ( $T_k$ ), toughness modulus after knot unfastening of knotted fibers ( $T_u'$ ), toughness modulus of reference unknotted samples ( $T_u$ ).

Material	Knot topology	Sample number	Strength [MPa]	Friction stress/strength	Toughness modulus, $T_k$ [J/g]	Toughness modulus after unfastening, $T_u'$ [J/g]	Toughness modulus, $T_u$ [J/g]
Raw silk	STSK	1	-	-	-	-	-
Raw silk	STSK	2	305	25.5%	67.7	-	32.6
Raw silk	STSK	3	246	29.0%	53.1	-	19.6
Raw silk	STSK	4	269	25.0%	52.1	23.1	
Raw silk	STSK	5	200	23.1%	37.1	-	8.5
Raw silk	STSK	6	196	38.6%	42.5	-	8.5
Raw silk	STSK	7	115	0.4%	3.5	2.6	-
Raw silk	STSK	8	226	1.0%	18.8	17.4	-
Raw silk	STSK	9	191	1.3%	22.1	20.4	-
Raw silk	STSK	10	220	6.2%	20.3	14.2	-
Raw silk	STSK	11	246	3.1%	25.1	21.8	-
Raw silk	STSK	12	183	30.2%	39.4	7.7	-
Raw silk	STSK	13	165	24.7%	27.8	7.3	-
Raw silk	STSK	14	-	-	-	-	-
Raw silk	STSK	15	269	5.1%	30.7	23.5	-
Raw silk	STSK	16	244	1.4%	13.6	11.9	-
Raw silk	STSK	17	242	4.1%	21.5	17.6	-
Raw silk	STSK	18	268	17.0%	41.7	22.9	-
Raw silk	STSK	19	191	6.8%	18.0	-	8.5

Supplementary Table S2. Raw silk fibers with double turned slip knot: Strength, average friction stress/strength over 0% - 40% of the strain at break, toughness modulus ( $T_k$ ), toughness modulus after knot unfastening of knotted fibers ( $T_u'$ ).

Material	Knot topology	Sample number	Strength [MPa]	Friction stress/strength	Toughness modulus, $T_k$ [J/g]	Toughness modulus after unfastening, $T_u'$ [J/g]
Raw silk	DTSK	1	235	0.1%	-	-
Raw silk	DTSK	2	297	0.0%	14.1	13.9
Raw silk	DTSK	3	312	0.5%	31.6	31.2
Raw silk	DTSK	4	171	0.1%	8.0	7.3
Raw silk	DTSK	5	243	0.5%	18.7	18.3
Raw silk	DTSK	6	175	0.6%	12.4	10.6
Raw silk	DTSK	7	-	-	-	-
Raw silk	DTSK	8	111	0.8%	-	-
Raw silk	DTSK	9	117	0.8%	-	-
Raw silk	DTSK	10	198	1.8%	-	-
Raw silk	DTSK	11	157	1.1%	-	-
Raw silk	DTSK	12	7	-	-	-
Raw silk	DTSK	13	236	0.9%	-	-
Raw silk	DTSK	14	226	0.5%	-	-
Raw silk	DTSK	15	212	0.5%	11.9	10.5
Raw silk	DTSK	16	219	0.4%	12.5	11.7
Raw silk	DTSK	17	267	0.2%	-	-
Raw silk	DTSK	18	209	0.4%	-	-
Raw silk	DTSK	19	273	0.4%	26.1	23.8

Supplementary Table S3. Degummed silk fibers with single turned slip knot: Strength, average friction stress/strength over 0% - 40% of the strain at break, toughness modulus ( $T_k$ ), toughness modulus after knot unfastening of knotted fibers ( $T_u'$ ).

Material	Knot topology	Sample number	Strength [MPa]	Friction stress/strength	Toughness modulus, $T_k$ [J/g]	Toughness modulus after unfastening, $T_u'$ [J/g]
Degummed silk	STSK	1	396	13.1%	27.3	8.4
Degummed silk	STSK	2	508	4.9%	48.0	34.4
Degummed silk	STSK	3	-	-	-	-
Degummed silk	STSK	4	325	1.4%	22.8	21.6
Degummed silk	STSK	5	675	0.6%	67.1	64.4
Degummed silk	STSK	6	452	3.0%	24.4	16.0
Degummed silk	STSK	7	410	9.0%	36.8	19.5
Degummed silk	STSK	8	401	6.0%	25.3	17.2
Degummed silk	STSK	9	-	-	-	-
Degummed silk	STSK	10	-	-	-	-
Degummed silk	STSK	11	420	7.5%	30.3	17.0
Degummed silk	STSK	12	223	8.2%	18.8	5.8

Supplementary Table S4. Degummed silk fibers with double turned slip knot: Strength, average friction stress/strength over 0% - 40% of the strain at break, toughness modulus ( $T_k$ ), toughness modulus after knot unfastening of knotted fibers ( $T_u'$ ).

Material	Knot topology	Sample number	Strength [MPa]	Friction stress/strength	Toughness modulus, $T_k$ [J/g]	Toughness modulus after unfastening, $T_u'$ [J/g]
Degummed silk	DTSK	1	-	-	-	-
Degummed silk	DTSK	2	-	-	-	-
Degummed silk	DTSK	3	225	0.5%	5.0	3.3
Degummed silk	DTSK	4	318	0.7%	15.5	10.8
Degummed silk	DTSK	5	518	0.0%	-	-
Degummed silk	DTSK	6	-	-	-	-
Degummed silk	DTSK	7	-	-	-	-
Degummed silk	DTSK	8	-	-	-	-
Degummed silk	DTSK	9	-	-	-	-
Degummed silk	DTSK	10	624	0.0%	32.6	31.0
Degummed silk	DTSK	11	-	-	-	-
Degummed silk	DTSK	12	-	-	-	-
Degummed silk	DTSK	13	-	-	-	-
Degummed silk	DTSK	14	455	2.2%	34.4	32.0
Degummed silk	DTSK	15	-	-	-	-
Degummed silk	DTSK	16	243	0.4%	7.2	4.9
Degummed silk	DTSK	17	-	-	-	-
Degummed silk	DTSK	18	370	0.6%	13.6	13.2
Degummed silk	DTSK	19	-	-	-	-
Degummed silk	DTSK	20	489	0.4%	35.1	34.1
Degummed silk	DTSK	21	497	0.2%	57.1	56.3
Degummed silk	DTSK	22	-	-	-	-
Degummed silk	DTSK	23	391	0.3%	22.2	21.1
Degummed silk	DTSK	24	-	-	-	-
Degummed silk	DTSK	25	-	-	-	-
Degummed silk	DTSK	26	-	-	-	-
Degummed silk	DTSK	27	470	0.8%	45.1	42.9
Degummed silk	DTSK	28	696	1.2%	47.0	42.8

Finally, some reference values of toughness modulus or strength of control raw or degummed single silk unknotted fibers (Supplementary Figures S1 and S2) are provided in Supplementary Tables S5 and S6, respectively. The average of the reported values were included in Table 1 in the main text.

Supplementary Table S5. Strength and toughness modulus of control raw silk unknotted fibers.

Material	Sample number	Diameter [ $\mu\text{m}$ ]	Strength [MPa]	Toughness modulus, $T_u$ [J/g]
Raw silk	1	21	271	32.6
Raw silk	2	20	251	19.6
Raw silk	3	21	179	8.5
Raw silk	4	19	315	36.2
Raw silk	5	22	236	27.1
Raw silk	6	25	171	18.1
Raw silk	7	18	231	18.1
Raw silk	8	19	97	4.1
	Mean	21	219	20.5
	St. Dev.	2	68	11.1

Supplementary Table S6. Strength and toughness modulus of control degummed silk unknotted fibers.

Material	Sample number	Diameter [ $\mu\text{m}$ ]	Strength [MPa]	Toughness modulus, $T_u$ [J/g]
Degummed silk	1	12	339	15.0
Degummed silk	2	8	646	43.5
Degummed silk	3	12	441	47.9
Degummed silk	4	12	415	17.6
Degummed silk	5	12	544	26.4
Degummed silk	6	14	490	24.8
Degummed silk	7	14	496	18.7
Degummed silk	8	14	474	40.1
	Mean	12	481	29.3
	St. Dev.	2	91	12.8

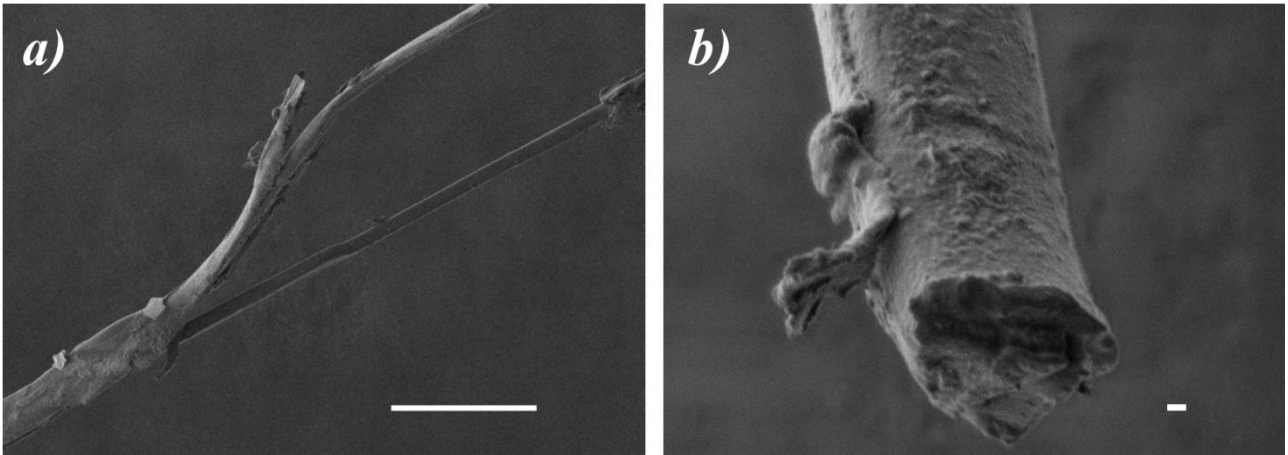


Figure S1: a) SEM image of a natural silk fiber (bave), where the seracin coating, which binds two core brins (detailed in b), scale bar: 1 μm), is broken (scale bar: 100 μm).

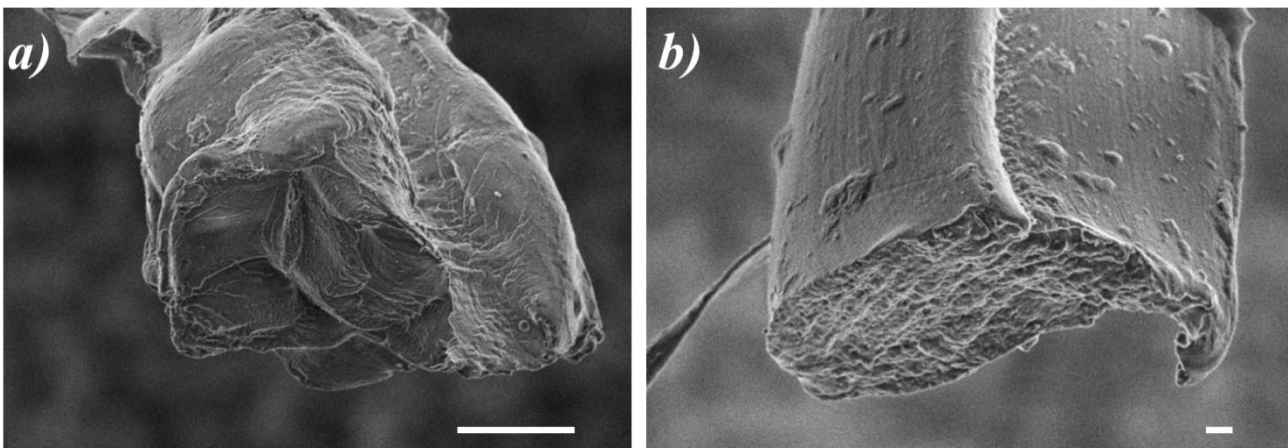


Figure S2: a) Cross-section of a natural silk fiber, consisting of two fibroin cores coated by a seracin layer (scale bar: 10 μm); b) Cross section of a degummed silk fiber (scale bar: 1 μm).

## References

[S1] Ashby MF, Elsevier 2011, Materials Selection in Mechanical Design Butterworth-Heinemann, Burlington, MA, USA.